UCLA
UCLA Previously Published Works

Title
Targeted Deletion and Lipidomic Analysis Identify Epithelial Cell COX-2 as a Major Driver of Chemically Induced Skin Cancer

Authors
Jiao, Jing
Ishikawa, Tomo-O
Dumlao, Darren S
et al.

Peer reviewed

Targeted Deletion and Lipidomic Analysis Identify Epithelial Cell COX-2 as a Major Driver of Chemically-induced Skin Cancer

Jing Jiao[1], **Tomo-o Ishikawa**[1,2], **Darren S. Dumlao**[3], **Paul C. Norris**[3], **Clara E. Magyar**[4], **Carol Mikulec**[5], **Art Catapang**[1], **Edward A. Dennis**[3], **Susan M. Fischer**[5], and **Harvey R. Herschman**[1]

[1]Departments of Molecular & Medical Pharmacology, and Biological Chemistry, University of California, Los Angeles, Los Angeles CA 90095

[3]Department of Chemistry and Biochemistry, Department of Pharmacology, University of California, San Diego, La Jolla, CA 92093

[4]Pathology and Laboratory Medicine, University of California, Los Angeles, Los Angeles, CA 90095

[5]University of Texas M.D. Anderson Cancer Center, Science Park, Smithville, TX 78957

Abstract

Pharmacologic and global gene deletion studies demonstrate that cyclooxygenase-2 (PTGS2/COX2) plays a critical role in DMBA/TPA-induced skin tumor induction. While many cell types in the tumor microenvironment express COX-2, the cell types in which COX-2 expression is required for tumor promotion are not clearly established. Here, cell-type specific *Cox-2* gene deletion reveals a vital role for skin epithelial cell COX-2 expression in DMBA/TPA tumor induction. In contrast, myeloid *Cox-2* gene deletion has no effect on DMBA/TPA tumorigenesis. The infrequent, small tumors that develop on mice with an epithelial cell-specific *Cox-2* gene deletion have decreased proliferation and increased cell differentiation properties. Blood vessel density is reduced in tumors with an epithelial cell-specific *Cox-2* gene deletion, compared to littermate control tumors, suggesting a reciprocal relationship in tumor progression between COX-2 expressing tumor epithelial cells and microenvironment endothelial cells. Lipidomics analysis of skin and tumors from DMBA/TPA-treated mice suggests that the prostaglandins PGE2 and PGF2α are likely candidates for the epithelial cell COX-2-dependent eicosanoids that mediate tumor progression. This study both illustrates the value of cell-type specific gene deletions in understanding the cellular roles of signal-generating pathways in complex microenvironments and emphasizes the benefit of a systems-based lipidomic analysis approach to identify candidate lipid mediators of biological responses.

Corresponding author: Harvey Herschman, 611 Charles E. Young Drive East, Los Angeles, CA 90095-1735. Phone: 310-825-8735; Fax: 310-825-1447; hherschman@mednet.ucla.edu.
[2]Present address: TransGenic. Inc. Kobe 650-0589, Japan

Keywords

COX-2; cyclooxygenase; DMBA/TPA-induced skin cancer; lipidomics

INTRODUCTION

Over three million non-melanoma skin cancers occur annually in the United States (1). Ease of monitoring has made mouse skin cancer a popular model to study cancer development (2). The most commonly used model is the "two stage" 7,12 dimethylbenz[a]anthracene (DMBA) "initiation"/12-*0*-tetradecanoylphorbol-13-acetate (TPA) "promotion" paradigm, resulting in papillomas "consisting of hyperplastic keratinocytes and supporting stroma" (3). A percentage of papillomas "progress" to squamous cell carcinomas (SCCs). "Initiation" results from *c-H-Ras* mutations in skin epithelial cells (3, 4); "promotion" is the TPA-driven clonal expansion of initiated keratinocytes to benign papilloma formation; "progression" is papilloma growth and conversion to SCCs (3, 5). Skin papillomas and SCCs can also be induced by repeated UVB-irradiation of SKH-1 hairless mice (6).

Prostaglandins (PGs) are derived from arachidonic acid. Arachidonate, released from plasma membrane phospholipids by phospholipases, is converted to PGH_2 by cyclooxygenase (COX) enzymes. PGH_2 is subsequently converted to prostanoids (e.g., PGE_2, PGD_2, PGI_2) by alternative prostanoid synthases (7). There are two *Cox* genes (8), *Cox-1* and *Cox-2* (7). Both COX-1 and COX-2 are inhibited by non-steroidal anti-inflammatory drugs (NSAIDs) (e.g. aspirin, indomethacin). COX-2 discovery prompted a search for selective inhibitors to reduce COX-1 inhibition adverse effects (e.g. gastric irritability; blood clotting inhibition), culminating in development of Coxibs (COX-2 selective inhibitors; e.g., Celebrex) (7).

COX-2 is overexpressed in many epithelial cancers (9, 10). COX-2 expression is *essential* for DMBA/TPA skin tumor induction; NSAID or Coxib treatment reduces tumor incidence and frequency (11). Global *Cox-2* gene deletion similarly reduces DMBA/TPA-induced tumors (12). UVB-induced skin cancer is also blocked by COX-2 inhibition (13) and by *Cox-2* deletion (14, 15).

Epithelial tumor cells live in a cellular microenvironment that includes fibroblasts, vasculature cells (e.g., endothelial cells, smooth muscle cells, pericytes), and immune cells (e.g., macrophages, lymphocytes, mast cells). The role of the "tumor microenvironment" in epithelial cancer development is a major topic in cancer research (16–18). COX-2 overproduction following DMBA/TPA treatment is reported in a variety of cell types, leading to the suggestion that COX-2 production in stromal/microenvironment cells modulates tumor progression (19). However, neither COX-2 inhibition nor *Cox-2* deletion can identify cell type(s) in which COX-2 expression is necessary for skin cancer development; both reduce COX-2 function in all cells. To determine COX-2 cell-specific roles we developed *Cox-2^flox* mice (20), in which *Cox-2* can be deleted with cell-type-specific Cre recombinase expression. Here we use *Cox-2^flox/flox* mice to determine the roles of skin keratinocyte- and myeloid cell-specific COX-2 expression in DMBA/TPA-induced skin tumorigenesis.

MATERIALS AND METHODS

Animals

Cox-$2^{flox/flox}$ (Cox-$2^{fl/fl}$); Cox-$2^{flox/flox}$;$K14Cre^{+}$ (Cox-2^{E}) and Cox-$2^{flox/flox}$;$LysMCre^{+}$ (Cox-2^{M}) mice, breeding and genotyping were described previously (20, 21). Animal experiments were performed with approval by the UCLA IACUC.

DMBA/TPA treatment

This procedure was described previously (22, 23). Briefly, female mice were initiated with a single application of 50 μg of DMBA (Sigma, Saint Louis MO). Two weeks after initiation, all groups received twice-weekly applications of 5 μg of TPA until the experiment was terminated. Tumor incidence (percent mice with tumors) and tumor multiplicity (papillomas/mouse) were determined weekly. Tumor incidence and multiplicity differences were analyzed by χ^2 tests and Mann-Whitney U, respectively.

Immunohistochemistry analyses

Skin and papilloma sections were fixed (4% paraformaldehyde), paraffin-embedded, sectioned (4 μm) and stained with hematoxylin and eosin (H&E) or processed for immunohistochemistry. Antigen retrieval was by heating (95°C in citrate buffer, pH 6.0) or Proteinase K (DAKO, Carpentaria, CA) treatment (37 °C). Antibodies are described in Supplemental Table 1. Samples were visualized with a NIKON Eclipse TE 2000-U microscope.

Epidermal thickness

Epidermal thickness (distance between basement lamina and apical surfaces of uppermost nucleated keratinocytes) (24) was measured on H&E sections. Measurements and quantification were performed with NIS-Elements BR 3.00 software (Nikon).

Quantification of immunohistochemical staining

Skin—Skin proliferation index: Ki67-positive basal cells/total basal cells. Premature basal cell differentiation index: Keratin 1 (K1)-positive basal cells/total basal keratinocytes.

Tumors—Morphometric analysis was performed with *Definiens'* Tissue Studio (Definiens Inc., Parsippany, NJ), using ScanScope AT instrumentation. Ki67-positive cells were determined with the pre-defined nuclear detection module and classification tool; positive and negative nuclei within each epithelial region were identified. Thresholds were set to classify hematoxylin stain for negative nuclei and DAB stain for positive nuclei. K1-positive epithelial cells/total epithelial cells and F4/80-positive macrophages/unit area were identified and quantified using the pre-defined cytoplasm detection module and classification tool. Blood vessel densities (vessels/unit area), based on CD31-positive staining, were determined with the pre-defined vessel detection module and classification tool. Data were analyzed using an unpaired Student's *t* test.

Eicosanoid profiling

Papillomas and skin samples were weighed, snap-frozen in liquid nitrogen and stored at −80 °C. Sample extraction and mass spectrometry were previously reported (25). An additional homogenization, using an Ultra-Turrax T25 Homogenizer (Fisher Scientific, Hampton, NH) was employed prior to solid-phase extraction. Samples thawed on ice were homogenized.

RESULTS

Epidermal keratinocyte *Cox-2* deletion reduces DMBA/TPA skin tumor induction

We observe COX-2 expression in DMBA/TPA-induced $Cox-2^{fl/fl}$ mice papillomas, and find macrophages present in these tumors (Fig. 1A). To examine the cell-specific role of keratinocyte COX-2 expression in DMBA/TPA skin cancer induction, we compared tumor induction in $Cox-2$ ^{E} mice (in which $Cox-2$ is deleted in keratinocytes, Supplemental Fig. S1) to tumor induction in $Cox-2^{fl/fl}$ littermates. Epithelial $Cox-2$ deletion significantly decreased tumor incidence in $Cox-2$ ^{E} mice; 59% of $Cox-2$ ^{E} mice developed papillomas. In contrast, 93% of $Cox-2^{fl/fl}$ mice developed papillomas (Fig. 1B; χ^2 test, $p<0.05$). Moreover, DMBA/TPA-induced papilloma multiplicity was reduced by nearly 80% in mice unable to express COX-2 in keratinocytes, when compared to $Cox-2^{fl/fl}$ mice (Fig. 1B, Mann-Whitney U test, $p<0.05$–0.001, week 11–20). Skin tumors that did develop on $Cox-2$ ^{E} mice were much smaller than tumors on $Cox-2^{fl/fl}$ mice (Fig. 2A).

Loss of one $Cox-2$ allele reduces, but does not eliminate, DMBA/TPA skin tumor induction (12). If incomplete Cre recombinase cleavage of floxed $Cox-2$ alleles in $Cox-2$ ^{E} mice occurs, these mice might develop heterozygous, COX-2-expressing tumors. Consequently, we analyzed COX-2 expression in papillomas from DMBA/TPA-treated $Cox-2^{fl/fl}$ and $Cox-2$ ^{E} mice. As expected, epithelial cells in papillomas from DMBA/TPA-treated $Cox-2^{fl/fl}$ mice express COX-2 protein (Fig. 2B). In contrast, COX-2 expression was undetectable in epithelial cells of papillomas from $Cox-2$ ^{E} mice (Fig. 2B). These data demonstrate that DMBA/TPA-induced tumors present on $Cox-2$ ^{E} mice are not COX-2 expression "escapees".

Myeloid cell *Cox-2* deletion has no effect on DMBA/TPA tumor induction

To investigate the role of myeloid cell COX-2 in DMBA/TPA-induced skin cancer we compared tumor induction in $Cox-2$ ^{M} mice and their $Cox-2^{fl/fl}$ littermates. To examine the efficiency of skin macrophage $Cox-2$ deletion in $Cox-2$ ^{M} mice, we isolated F4/80$^+$ skin macrophages from TPA-treated $Cox-2$ ^{M} and $Cox-2^{fl/fl}$ mice, and demonstrated that F4/80$^+$ skin macrophage from $Cox-2$ ^{M} mice undergo effective $Cox-2$ deletion (Supplemental Fig. S2). DMBA/TPA-treated $Cox-2$ ^{M} mice and $Cox-2^{fl/fl}$ littermates have no significant differences detectable in tumor incidence, multiplicity or size (Figs. 1C, 2A). Tumors from both $Cox-2$ ^{M} and $Cox-2^{fl/fl}$ mice demonstrated extensive COX-2 expression in epithelial cells of papillomas (Fig. 2B).

DMBA/TPA-induced skin hyperplasia is reduced *in Cox-2* ^{E} mice

Repeated TPA treatment causes mouse skin epidermal hyperplasia. However, global $Cox-2$ deletion reduced TPA-induced hyperplasia, when compared to $Cox-2^{+/+}$ mice (12). To

determine if reduced hyperplasia in DMBA/TPA-treated skin is an epithelial cell-intrinsic COX-2-mediated phenotype, we examined the effect of DMBA/TPA treatment on epidermal hyperplasia in *Cox-2* ^{E} and *Cox-2$^{fl/fl}$* mice.

Skin morphology is similar for untreated *Cox-2* ^{E} and *Cox-2$^{fl/fl}$* mice (Fig. 3A) and for *Cox-2* ^{M} mice and *Cox-2$^{fl/fl}$* mice (Fig. 3B). After DMBA initiation and 20 weeks of TPA treatment, skin of *Cox-2* ^{E} mice exhibits significantly reduced hyperplasia (i.e., epidermal thickness) when compared to skin of similarly treated *Cox-2$^{fl/fl}$* mice (Fig. 3A). A short two-week TPA treatment following DMBA initiation also led to decreased epidermal hyperplasia in *Cox-2* ^{E} mice (Supplemental Fig. S3A). No skin papillomas are present at this time (Fig. 1B). In contrast to reduced hyperplasia in *Cox-2* ^{E} mice (Fig. 3A), skin of *Cox-2* ^{M} mice and *Cox-2$^{fl/fl}$* littermates undergo similar degrees of DMBA/TPA-induced hyperplasia (Fig. 3B).

Epidermal keratinocyte-specific *Cox-2* deletion does not affect DMBA/TPA-induced epidermal cell proliferation, but induces aberrant epidermal differentiation

As basal cells move to suprabasal locations, they cease proliferation and undergo terminal differentiation. The balance between keratinocyte proliferation and differentiation is critical to maintain epidermal homeostasis (26). To investigate whether the reduced skin hyperplasia of *Cox-2* ^{E} mice following chronic, repeated TPA treatment (Fig. 3A) may result from decreased keratinocyte proliferation, the Ki67 marker for proliferating cells was examined in skin from untreated mice and mice treated for 20 weeks with chronic, repeated TPA stimulation. Skin of untreated *Cox-2* ^{E} mice and *Cox-2$^{fl/fl}$* littermates have very few Ki67 positive cells (Fig. 4A). Repeated TPA exposure induces substantial proliferation in skin of both mouse strains (Fig. 4A). However, there is no detectable difference in Ki67 expression frequency in skin basal cells of DMBA/TPA-treated *Cox-2* ^{E} mice and *Cox-2$^{fl/fl}$* littermates (Fig. 4B).

Keratin 1 is expressed in keratinocytes as they commit to differentiation (27). Untreated skin from mice with a keratinocyte-specific *Cox-2* deletion and their *Cox-2$^{fl/fl}$* littermates have similar low K1 antigen expression levels in suprabasal epidermal cells (Fig. 4C). Global *Cox-2* deletion results in premature differentiation in epidermal basal cells after DMBA/TPA treatment, when compared to *Cox-2$^{+/+}$* mice (12). Skin of DMBA/TPA-treated *Cox-2* ^{E} mice shows a greater than threefold increase in K1-positive basal cells relative to skin of DMBA/TPA-treated *Cox-2$^{fl/fl}$* littermates (Figs. 4C, 4D); the basal cell population undergoes premature terminal differentiation in *Cox-2* ^{E} mice but not in *Cox-2$^{fl/fl}$* littermates.

In addition to proliferation and differentiation, apoptosis can potentially contribute to epidermal homeostasis (28). However, apoptosis was minimal in skin from both untreated *Cox-2* ^{E} and *Cox-2$^{fl/fl}$* mice, and was not substantially increased in skin from DMBA/TPA-treated mice of either strain (Supplemental Fig. S4).

DMBA/TPA-induced papillomas of *Cox-2*^{E} mice have a decreased proliferation index

The increase in proliferation of skin epidermal cells in response to DMBA/TPA treatment is similar *Cox-2*^{E} and *Cox-2*$^{fl/fl}$ littermates (Fig. 4B). However, papillomas on DMBA/TPA-treated *Cox-2*^{E} mice are smaller than those on their *Cox-2*$^{fl/fl}$ littermates (Fig. 2A). These observations raised the question of whether, unlike in skin, proliferation indices of papillomas present on *Cox-2*^{E} mice are reduced relative to proliferation indices of papillomas present on *Cox-2*$^{fl/fl}$ littermates. Ki67 proliferation indices for DMBA/TPA-induced *Cox-2*^{E} papillomas were two-fold lower than proliferation rates of *Cox-2*$^{fl/fl}$ littermate papillomas (Fig. 5A). The data suggest that, once initial promotion event(s) for DMBA/TPA-induced papillomas occur in skin of *Cox-2*^{E} mice, proliferation may become a rate-limiting step in tumor progression. In contrast, myeloid cell *Cox-2* deletion had no discernable effect on tumor cell proliferation in DMBA/TPA-induced papillomas (Fig. 5A).

Epithelial cells of DMBA/TPA-induced papillomas from *Cox-2*^{E} mice exhibit increased differentiation

Loss of cell differentiation is generally associated with cancer progression; reduced K1 expression is associated with DMBA/TPA-induced skin progression (5). Conversely, induced tumor cell differentiation is thought to retard cancer progression (29–32). Premature basal cell differentiation in DMBA/TPA-treated mouse skin, previously demonstrated to be a property of mice with a global *Cox-2* deletion (12), is an intrinsic property of the epidermal tumor precursor cell, occurring in *Cox-2*^{E} mice (Figs. 4C, 4D). These data suggest that a tendency to premature differentiation, as a result of loss of intrinsic epithelial cell COX-2 expression, may modulate proliferation of the transformed skin epithelial tumor cell. Loss of COX-2 expression in epithelial tumor cells of *Cox-2*^{E} mice resulted in DMBA/TPA-induced tumors that exhibit two-fold increased differentiation, as measured by increased numbers of basal cells expressing K1 (Fig. 5B). In contrast, myeloid *Cox-2* deletion in *Cox-2*^{M} mice had no detectable effect on epithelial tumor cell differentiation (Fig. 5B).

An increase in apoptosis of epithelial tumor cells in the DMBA/TPA-induced papillomas on *Cox-2*^{E} mice, relative to apoptosis in tumors on *Cox-2*$^{fl/fl}$ mice, could also contribute to the reduced tumor progression observed in *Cox-2*^{E} mice. However, apoptotic cells were very sparse both in tumors of *Cox-2*^{E} mice and their *Cox-2*$^{fl/fl}$ littermates (Supplemental Fig. S4), and quantifiable differences could not be demonstrated.

Eicosanoid profiles of skin and skin tumors from DMBA/TPA-treated *Cox-2*^{E} mice, *Cox-2*^{M} mice, and their *Cox-2*$^{fl/fl}$ littermates

DMBA/TPA-induced skin tumors have within them epithelial cells, macrophages, endothelial cells, fibroblasts and other stromal and immune cells. The targeted *Cox-2* deletions described here eliminate one of the two cyclooxygenases, COX-2, in single cell types (epithelial keratinocytes or myeloid cells) of the tumors. By analyzing total tumor eicosanoid profiles, one can determine whether the absence of COX-2 only in epithelial tumor cells, or only in myeloid cells, will alter significantly polyunsaturated fatty acid metabolism in DMBA/TPA-induced skin cancer; i.e., measuring total eicosanoids will allow us to address the question "to what extent does either keratinocyte-specific COX-2 or

myeloid-specific COX-2 contribute to eicosanoid metabolism in DMBA/TPA-induced skin tumors?"

We developed a comprehensive lipidomic approach for complete extraction of tissue eicosanoids, combined with high-throughput LC/MS/MS methodology to quantify multiple eicosanoid species (25). We collected, from all four groups of mice (*Cox-2* [E] and their *Cox-2*^{fl/fl} littermates, and *Cox-2* [M] and their *Cox-2*^{fl/fl} littermates), (i) untreated skin, (ii) DMBA/TPA-treated skin and (iii) papillomas from DMBA/TPA-treated mice. Eicosanoid extracts were analyzed by high throughput mass spectrometry, using MRM scanning (25).

Despite profound differences in tumor incidence, frequency and size for tumors of *Cox-2* [E] mice when compared to tumors of their *Cox-2*^{fl/fl} littermates (Figs. 1B, 2A), no statistically significant differences in total eicosanoid amounts present in tumors from these mice was detectable (Fig. 6A). Similarly, there is no detectably significant difference in total eicosanoid content in DMBA/TPA-induced skin tumors from *Cox-2* [M] mice and their *Cox-2*^{fl/fl} littermates (Fig. 6A).

Complete lipidomic analysis allows comparison of COX-dependent product levels, non-enzymatic eicosanoids, lipoxygenase-dependent products (LOX), and cytochrome P450 products (CYP) in the tumor sets. LOX products, which constitute the majority of tumor eicosanoid metabolites (Fig. 6B), do not differ in total mass when comparisons are made between tumors from experimental and littermate control mice; no statistically significant differences were detected. However, although the amounts of COX-dependent eicosanoids is perhaps surprisingly low, a small but statistically significant reduction in total COX-dependent eicosanoids occurs in the tumors of *Cox-2* [E] mice, when compared with tumors from their *Cox-2*^{fl/fl} littermates (Fig. 6B). In contrast, myeloid cell *Cox-2* deletion had no effect on total COX-dependent eicosanoids in DMBA/TPA-induced tumors (Fig. 6B).

The decrease in COX-dependent eicosanoids in *Cox-2* [E] mice (Fig. 6B) suggests that an epithelial-specific COX-2-dependent product(s), absent in tumors of these mice but present in tumors of their *Cox-2*^{fl/fl} littermates, may be responsible for the differences in tumor number and progression observed in *Cox-2* [E] mice and their *Cox-2*^{fl/fl} littermates (Fig. 1B, Fig. 2A). COX products whose levels are reduced in *Cox-2* [E] tumors, but not in tumors of the other mouse genotypes, are likely to include candidates for the keratinocyte-specific COX-2 product(s) that drives DMBA/TPA-induced tumors. A "heat map" (Fig. 6C), identifies those COX-dependent products that are significantly reduced in tumors of *Cox-2* [E] mice versus their *Cox-2*^{fl/fl} littermates, and compares these data with the (lack of) changes in levels of these same eicosanoids in *Cox-2* [M] mice and their *Cox-2*^{fl/fl} littermates.

To identify COX-2-dependent prostanoids that are likely candidates as causal drivers in COX-2-dependent DMBA/TPA tumor proliferation/progression, we compared levels of the COX-2-dependent eicosanoids reduced in papillomas from *Cox-2* [E] mice relative to their *Cox-2*^{fl/fl} littermates (Fig. 6C) with the levels of those same eicosanoids in skin samples from the same DMBA/TPA-treated mice. Our hypothesis was that epithelial-cell COX-2-dependent prostanoids causal for tumor progression would be decreased in tumors from *Cox-2* [E] mice relative to their *Cox-2*^{fl/fl} littermates; that the keratinocyte COX-2-dependent

eicosanoids that drive tumor progression would (i) be elevated in tumors from $Cox\text{-}2^{fl/fl}$ mice and (ii) be reduced, in tumors in $Cox\text{-}2^{E}$ mice, to levels similar to skin samples from these mice. As additional supporting evidence we proposed that the presumptive epithelial cell COX-2-dependent eicosanoids that drive DMBA/TPA tumor progression would be elevated in DMBA/TPA-induced tumors from both $Cox\text{-}2^{M}$ mice and their $Cox\text{-}2^{fl/fl}$ littermates, relative to these eicosanoids in skin from $Cox\text{-}2^{E}$ mice.

The two COX-2-dependent eicosanoids that meet the above criteria are PGE_2 and $PGF_{2\alpha}$ (Fig. 6D). For both PGE_2 and $PGF_{2\alpha}$ (i) levels are elevated in tumors of DMBA/TPA-treated $Cox\text{-}2^{fl/fl}$ mice when compared to levels in skin of DMBA/TPA-treated $Cox\text{-}2^{fl/fl}$ mice, (ii) levels in the $Cox\text{-}2^{E}$ DMBA/TPA-induced tumors are reduced to levels not significantly different from that of DMBA/TPA-treated skin (Fig. 6D) and (iii) levels are not reduced in tumors of $Cox\text{-}2^{M}$ mice, when compared to tumors of their $Cox\text{-}2^{fl/fl}$ controls (Fig. 6D). Either (or both) of these intrinsic keratinocyte COX-2-dependent eicosanoids is/are likely to be a major driver(s) of DMBA/TPA-induced tumor promotion/progression. Although we observe statistically significant differences in non-enzymatically derived eicosanoids and CYP-derived eicosanoids, functional significance of these eicosanoids to DMBA/TPA-induced tumorigenesis is not clear.

There were no detectable differences in PGE_2 and $PGF_{2\alpha}$ levels in DMBA/TPA-treated skin of $Cox\text{-}2^{E}$ and their $Cox\text{-}2^{fl/fl}$ littermates, although – in both cohorts – repeated TPA treatment did substantially increase levels of the two eicosanoids when compared to untreated skin (Fig. 6D). Additional COX-2 IHC studies suggested that, while a single TPA application to mouse skin significantly increased epithelial COX-2 levels, long-term repeated TPA treatment does not lead to elevated COX-2 expression in the skin (Supplemental Fig. S5), as previously reported by Muller-Decker et al (33). However, papillomas from the same mouse show elevated COX-2 expression relative to adjacent skin.

DMBA/TPA-induced papillomas of $Cox\text{-}2^{E}$ mice exhibit reduced vascularity

The most parsimonious explanation for reduced DMBA/TPA skin tumor induction in $Cox\text{-}2^{E}$ mice is that the critical epithelial cell COX-2-dependent prostanoids act intrinsically on the same cell that produces them. In the absence of these epithelial cell-specific, COX-2-dependent prostanoids and their intrinsic autocrine modulatory effect on the initiated epithelial cell, proliferation is decreased and differentiation is increased, resulting in reduced tumor progression.

However, it is also possible, and even likely, that COX-2-dependent prostanoids secreted by DMBA/TPA-induced tumor cells act on other cells in the tumor microenvironment. As a consequence, these cells modulate proliferation, differentiation and additional properties of the epithelial tumor cells in a reciprocal relationship that modifies tumor promotion/ progression. Among the cells in the tumor microenvironment thought to modulate tumor proliferation/progression are infiltrating macrophages and endothelial cells for blood vessel formation (34, 35). To investigate possible epithelial cell-specific COX-2-dependent prostanoid modulation of extrinsic cells in the tumor microenvironment we evaluated (i) macrophage migration into tumors of $Cox\text{-}2^{E}$ mice and their $Cox\text{-}2^{fl/fl}$ littermates and into

tumors of *Cox-2* ^{M} mice and their *Cox-2$^{fl/fl}$* littermates, and (ii) tumor blood vessel densities in these four mouse cohorts.

Macrophage infiltration was evaluated by quantitative F4/80^{+} cell density determination in tumors (Fig. 7A). Despite differences in tumor incidence, multiplicity and size, macrophage densities in tumors from *Cox-2* ^{E} and *Cox-2$^{fl/fl}$* littermates were not significantly different (Fig. 7A). Moreover, macrophage densities in *Cox-2* ^{M} mice and *Cox-2$^{fl/fl}$* littermates were also similar to one another. *Cox-2* deletion in *Cox-2* ^{E} mice and in *Cox-2* ^{M} mice had no significant effect on numbers of macrophage present in DMBA/TPA-induced papillomas.

Papilloma vascularity was also measured in tumors of *Cox-2* ^{E} and *Cox-2$^{fl/fl}$* littermates. Vessel density in *Cox-2* ^{E} tumors was reduced by over 50% when compared to *Cox-2$^{fl/fl}$* tumors (Fig. 7B), suggesting that that keratinocyte-specific, COX-2-dependent prostanoid production modulates blood vessel density in DMBA/TPA-induced tumors. Moreover, the papillomas derived from *Cox-2* ^{E} mice have an increased percentage of small vessels and a correspondingly decreased percentage of (medium-size + large-size) vessels, when compared to vessels formed in tumors of *Cox-2$^{fl/fl}$* mice (Supplemental Fig. S6). In contrast, no significant difference in blood vessel density or size distribution was observable in tumors from *Cox-2* ^{M} and *Cox-2$^{fl/fl}$* littermate mice (Fig. 7B, Supplemental Fig. S6).

DISCUSSION

COX-2 overexpression occurs in many epithelial tumors and is suggested to play a modulatory role in many cancers. However, COX-2 expression occurs in tumor epithelial cells and also in other cell types within the tumor microenvironment. Although COX-2 inhibitor and global *Cox-2* deletion studies provide unequivocal evidence that COX-2 plays a major role in driving DMBA/TPA-induced mouse skin cancer, one cannot determine the causal effects of COX-2-dependent prostanoids from different cell types either by pharmacological or by global gene knockout approaches; both procedures eliminate COX-2 activity in all cell types. Here, using cell-type specific *Cox-2* deletion, we demonstrate a requirement for intrinsic epithelial keratinocyte COX-2 expression in DMBA/TPA-induced skin cancer progression. In addition, we demonstrate that myeloid COX-2 expression has no significant role in DMBA/TPA-inducd skin cancer development.

To address the role of epithelial cell COX-2 in skin cancer formation, we ablated the *Cox-2* gene using mice expressing *K14-Cre*. K14 is expressed in skin by E14.5 (36). K14-Cre is expressed in progenitor cells in the basal layer and hair follicular bulge stem cells (36) and can successfully label skin cancer stem cells, using a genetic lineage tracing system (37). Consequently, skin epithelial cells and their precursors in *Cox-2* ^{E} mice will be deleted for COX-2 expression, as will the tumor cells derived from cancer stem cells.

Lao et al (38) approached the role of autonomous COX-2 expression for *Ras*-initiated epithelial cells in tumorigenesis in a different manner; they transformed *Cox-2$^{+/+}$* and *Cox-2$^{-/-}$* keratinocytes with a v-H-*Ras* retrovirus and analyzed the ability of the transformed cells to form tumors following cutaneous orthografting onto athymic, immunodeficient mice. After four weeks, tumor incidence was reduced ~25% and tumor

size was reduced ~60% for Cox-$2^{-/-}$ Ras- transformed keratinocyte orthografts. Their data, like our own, support the conclusion that intrinsic COX-2 expression in skin epithelial cells bearing an oncogenic Ras gene plays a major role in driving skin tumor promotion. However, tumor formation in their experiment is really "one stage"; the v-H-Ras transformed keratinocytes form tumors without requiring a promotion stimulus. In contrast, Brown et al (39) directly transfected mouse skin with v-H-Ras retrovirus and demonstrated (i) no tumor formation occurred in response to viral administration and (ii) subsequent TPA treatment elicited papilloma formation.

Both skin tumors produced by engrafted v-H-$Ras;Cox$-$2^{-/-}$ keratinocytes (38) and skin tumors on DMBA/TPA-treated Cox-2^{E} mice demonstrate reduced proliferation and increased terminal differentiation when compared to their Cox-$2^{+/+}$ counterparts, suggesting tumor cell-autonomous COX-2 expression plays an important role in modulating these skin tumor characteristics. The most parsimonious explanation for these results is that COX-2-dependent prostanoids produced by epithelial tumor cells play a cell-autonomous role in driving tumor cell proliferation and retarding tumor cell differentiation. However, Lao et al (38) find no difference in tumor vascularization in v-H-$Ras; Cox$-$2^{+/+}$ and v-H-Ras;Cox-$2^{-/-}$ keratinocyte-derived tumors (38), while we find a two-fold difference in tumor vascularization between DMBA/TPA-induced tumors present on Cox-2^{E} mice versus their Cox-$2^{fl/fl}$ littermates (Fig. 7B). Our data suggest (i) that skin epithelial tumor cell COX-2-dependent prostanoids may also modulate biological properties of other cell types in their microenvironment and (ii) that, as a consequence, cells of the microenvironment may then reciprocally respond to tumor cell COX-2-dependent prostanoids to subsequently modulate tumor development.

Additional differences between the Lao et al study (38) and our own that may influence tumor formation are (i) the number of initiated cells from which tumors arise; Lao et al (38) engraft 3×10^6 v-H-Ras-transformed keratinocytes at a single site, while tumors in our experiment likely develop from individual Ras- initiated cells, (ii) differences in the biology of keratinocytes transformed by v-H-Ras retrovirus in culture and mutated c-H-Ras-initiated cells, and (iii) lack of an immune system in the engrafted athymic immunodeficient mouse for what is thought to be an inflammation-driven process. In addition, we note differences in time to detectable tumor formation; less than two weeks for Lao et al (38) versus six to eight weeks for DMBA/TPA-induced tumors (22, 23).

The most direct reconciliation of the Lao et al data (38) and our own suggest v-H-Ras-transformed keratinocytes, capable of rapidly forming tumors in the absence of promotion but dependent on COX-2 expression (38), may reflect skin keratinocytes from DMBA/TPA-treated mice that have transitioned to intrinsic COX-2 dependence in the two-stage carcinogenesis model. Both experiments *do* converge on the requirement for intrinsic COX-2 expression in skin epithelial cells for robust tumor formation.

We observe a ~10-fold increase in PGE_2 and $PGF_{2\alpha}$ (Fig. 6D) in the skin of both DMBA/TPA–treated Cox-2^{E} and Cox-$2^{fl/fl}$ mice, relative to the skin of untreated mice. Tiano et al (12) observed a qualitatively similar result for PGE_2 levels in DMBA/TPA-treated global Cox-$2^{-/-}$ mice and their Cox-$2^{+/+}$ controls. The data suggest that the elevated prostanoid

levels observed in DMBA/TPA-chronically treated skin are *not* dependent on keratinocyte COX-2 production. In contrast, global *Cox-1* deletion, which also greatly reduces DMBA/TPA skin tumor induction, significantly reduces skin PGE_2 levels in DMBA/TPA-treated mice (12). These data suggest (i) that COX-1 expression in skin of DMBA/TPA-treated mice is likely to play a role in TPA-driven progression of DMBA-initiated cells to papillomas and (ii) that elevated COX-2 expression in initiated keratinocytes is necessary, *at some point(s)*, for transition to a detectable papilloma.

Like Muller-Decker *et al.* (33), we observe COX-2 expression in papillomas of DMBA/TPA-treated mice, but not in adjacent skin (Supplemental Fig. S5). Moreover, using heterozygous mice in which a luciferase reporter is substituted for the coding region of the *Cox-2* gene in one allele, elevated luciferase expression is detectable as soon as a visible DMBA/TPA-induced papilloma is present, but not prior to this point (22). These data suggest that elevated COX-2 expression in skin epithelial cells is required at, and subsequent to, this point in time for DMBA/TPA-driven papilloma appearance and progression, but may not be required prior to this point for subsequent tumor production. There appears to be a TPA-induced, but epithelial/keratinocyte COX-2 independent event(s) that occurs in DMBA-initiated skin. However, TPA-dependent, increased epithelial cell COX-2 expression is required for DMBA/TPA tumor induction. The data suggest that, in skin of DMBA/TPA-treated mice, epithelial cells may undergo a "pre-progression" event (or events) that is (are) not dependent on epithelial keratinocyte COX-2 prostanoid production. Once this pre-progression event(s) is completed, the cells become committed to a transition to papilloma formation; this transition requires increased COX-2 production in the initiated skin epithelial cell.

Tumor promotion is stunted in the absence of an increase in COX-2 expression in initiated epithelial cells; COX-2 elevation in DMBA/TPA-treated epithelial cells is required for sustained tumor promotion. The smaller, less frequent tumors observed on DMBA/TPA-treated *Cox-2*^{E} mice (Figs. 1 and 2) may reflect the beginning, but relatively unsuccessful, proposed epithelial cell COX-2-dependent transition.

Identification of prostanoids that mediate DMBA/TPA-induced skin tumor progression has been primarily of the "candidate prostanoid" approach (12). PGE_2 (40) and $PGF_{2\alpha}$ (41) have emerged as the prostaglandins thought to modulate DMBA/TPA-induced skin cancer. Our unbiased analysis of arachidonic acid metabolites present in untreated skin, DMBA/TPA-treated skin and DMBA/TPA-induced papillomas of *Cox-2*^{E} and *Cox-2*$^{fl/fl}$ mice demonstrates that PGE_2 and $PGF_{2\alpha}$ are, indeed, the strongest candidates for transformed epithelial cell COX-2-derived prostaglandins that drive DMBA/TPA skin cancer; PGE_2 and $PGF_{2\alpha}$ levels of the less frequent, smaller papillomas of *Cox-2*^{E} mice are substantially lower than those of papillomas on *Cox-2*$^{fl/fl}$ littermates, and are similar to PGE_2 values found in adjacent skin. Interestingly, $PGF_{2\alpha}$ but not PGE_2, can reverse the inhibition of Indomethacin for DMBA/TPA skin tumor induction (33).

We suggest it is only by targeted, cell type-specific deletion of COX-2 expression and targeted cell type-specific deletion of appropriate prostaglandin receptors that the complex network of tumor cell autonomous and extrinsic cell COX-2-dependent prostanoid signaling

in skin tumor progression can be completely elucidated. Without such studies, speculation of cell-specific roles in skin cancer promotion and progression, both for COX-2-dependent prostanoid production and for responses to COX-2-dependent prostanoid cell stimulation, cannot be tested and either validated or refuted. Moreover, this argument for necessity of cell-specific inactivation of critical genes can be generalized to most considerations of cell-cell interactions in complex microenvironments, if either more than one cell type expresses the signaling molecule in question or if more than one cell type expresses a capacity to respond to the signal.

Supplementary Material

Refer to Web version on PubMed Central for supplementary material.

Acknowledgments

References

1. Donaldson MR, Coldiron BM. No end in sight: the skin cancer epidemic continues. Semin Cutan Med Surg. 2011; 30:3–5. [PubMed: 21540015]

2. Schwarz M, Munzel PA, Braeuning A. Non-melanoma skin cancer in mouse and man. Arch Toxicol. 2013; 87:783–798. [PubMed: 23266722]

3. Kemp CJ. Multistep skin cancer in mice as a model to study the evolution of cancer cells. Seminars in cancer biology. 2005; 15:460–473. [PubMed: 16039870]

4. Balmain A, Brown K. Oncogene activation in chemical carcinogenesis. Adv Cancer Res. 1988; 51:147–182. [PubMed: 3066145]

5. Abel EL, Angel JM, Kiguchi K, DiGiovanni J. Multi-stage chemical carcinogenesis in mouse skin: fundamentals and applications. Nat Protoc. 2009; 4:1350–1362. [PubMed: 19713956]

6. Benavides F, Oberyszyn TM, VanBuskirk AM, Reeve VE, Kusewitt DF. The hairless mouse in skin research. J Dermatol Sci. 2009; 53:10–18. [PubMed: 18938063]

7. Wang D, Dubois RN. Eicosanoids and cancer. Nat Rev Cancer. 2010; 10:181–193. [PubMed: 20168319]

8. Herschman, HR. Historical aspects of COX-2; cloning and chracterization of the cDNA, protein and gene. In: Harris, RE., editor. COX-2 Blockade in Cancer Prevention and Therapy. Totowa: Humana; 2003. p. 13-32.

9. Wang D, Dubois RN. Prostaglandins and cancer. Gut. 2006; 55:115–122. [PubMed: 16118353]

10. Anderson, WF.; Umar, A.; Vine, JL.; Hawk, ET. Potential role of NSAIDs and COX-2 blockade in cancer therapy. In: Harris, RE., editor. COX-2 blockade in cancer prevention and therapy. Totowa: Humana; 2003. p. 313-340.

11. Chun KS, Kundu JK, Park KK, Chung WY, Surh YJ. Inhibition of phorbol ester-induced mouse skin tumor promotion and COX-2 expression by celecoxib: C/EBP as a potential molecular target. Cancer Res Treat. 2006; 38:152–158. [PubMed: 19771276]

12. Tiano HF, Loftin CD, Akunda J, Lee CA, Spalding J, Sessoms A, et al. Deficiency of either cyclooxygenase (COX)-1 or COX-2 alters epidermal differentiation and reduces mouse skin tumorigenesis. Cancer Res. 2002; 62:3395–3401. [PubMed: 12067981]

13. Fischer SM, Lo HH, Gordon GB, Seibert K, Kelloff G, Lubet RA, et al. Chemopreventive activity of celecoxib, a specific cyclooxygenase-2 inhibitor, and indomethacin against ultraviolet light-induced skin carcinogenesis. Mol Carcinog. 1999; 25:231–240. [PubMed: 10449029]

14. Fischer SM, Pavone A, Mikulec C, Langenbach R, Rundhaug JE. Cyclooxygenase-2 expression is critical for chronic UV-induced murine skin carcinogenesis. Mol Carcinog. 2007; 46:363–371. [PubMed: 17219415]

15. Rundhaug JE, Fischer SM. Cyclo-oxygenase-2 plays a critical role in UV-induced skin carcinogenesis. Photochem Photobiol. 2008; 84:322–329. [PubMed: 18194346]

16. Allen M, Louise Jones J. Jekyll and Hyde: the role of the microenvironment on the progression of cancer. J Pathol. 2011; 223:162–176. [PubMed: 21125673]

17. Whiteside TL. The tumor microenvironment and its role in promoting tumor growth. Oncogene. 2008; 27:5904–5912. [PubMed: 18836471]

18. Polyak K, Haviv I, Campbell IG. Co-evolution of tumor cells and their microenvironment. Trends Genet. 2009; 25:30–38. [PubMed: 19054589]

19. Muller-Decker K, Neufang G, Berger I, Neumann M, Marks F, Furstenberger G. Transgenic cyclooxygenase-2 overexpression sensitizes mouse skin for carcinogenesis. Proc Natl Acad Sci U S A. 2002; 99:12483–12488. [PubMed: 12221288]

20. Ishikawa TO, Herschman HR. Conditional knockout mouse for tissue-specific disruption of the cyclooxygenase-2 (Cox-2) gene. Genesis. 2006; 44:143–149. [PubMed: 16496341]

21. Ishikawa TO, Oshima M, Herschman HR. Cox-2 deletion in myeloid and endothelial cells, but not in epithelial cells, exacerbates murine colitis. Carcinogenesis. 2011; 32:417–426. [PubMed: 21156970]

22. Ishikawa TO, Jain NK, Herschman HR. Cox-2 gene expression in chemically induced skin papillomas cannot predict subsequent tumor fate. Mol Oncol. 2010; 4:347–356. [PubMed: 20599447]

23. Ishikawa TO, Kumar IP, Machado HB, Wong KP, Kusewitt D, Huang SC, et al. Positron emission tomography imaging of DMBA/TPA mouse skin multi-step tumorigenesis. Mol Oncol. 2010; 4:119–125. [PubMed: 20171942]

24. Kietzmann M, Lubach D, Heeren HJ. The mouse epidermis as a model in skin pharmacology: influence of age and sex on epidermal metabolic reactions and their circadian rhythms. Lab Anim. 1990; 24:321–327. [PubMed: 2270041]

25. Dumlao DS, Buczynski MW, Norris PC, Harkewicz R, Dennis EA. High-throughput lipidomic analysis of fatty acid derived eicosanoids and N-acylethanolamines. Biochim Biophys Acta. 2011; 1811:724–736. [PubMed: 21689782]

26. Fuchs E. Finding one's niche in the skin. Cell Stem Cell. 2009; 4:499–502. [PubMed: 19497277]

27. Zhu S, Oh HS, Shim M, Sterneck E, Johnson PF, Smart RC. C/EBPbeta modulates the early events of keratinocyte differentiation involving growth arrest and keratin 1 and keratin 10 expression. Mol Cell Biol. 1999; 19:7181–7190. [PubMed: 10490653]

28. Fu W, McCormick T, Qi X, Luo L, Zhou L, Li X, et al. Activation of P2X(7)-mediated apoptosis Inhibits DMBA/TPA-induced formation of skin papillomas and cancer in mice. BMC Cancer. 2009; 9:114. [PubMed: 19379509]

29. Descargues P, Sil AK, Karin M. IKKalpha, a critical regulator of epidermal differentiation and a suppressor of skin cancer. Embo J. 2008; 27:2639–2647. [PubMed: 18818691]

30. von Wangenheim KH, Peterson HP. The role of cell differentiation in controlling cell multiplication and cancer. J Cancer Res Clin Oncol. 2008; 134:725–741. [PubMed: 18414896]

31. Li Q, Sambandam SA, Lu HJ, Thomson A, Kim SH, Lu H, et al. 14-3-3sigma and p63 play opposing roles in epidermal tumorigenesis. Carcinogenesis. 2011; 32:1782–1788. [PubMed: 21926108]

32. Botrugno OA, Santoro F, Minucci S. Histone deacetylase inhibitors as a new weapon in the arsenal of differentiation therapies of cancer. Cancer Lett. 2009; 280:134–144. [PubMed: 19345000]

33. Muller-Decker K, Scholz K, Marks F, Furstenberger G. Differential expression of prostaglandin H synthase isozymes during multistage carcinogenesis in mouse epidermis. Mol Carcinog. 1995; 12:31–41. [PubMed: 7818763]

34. Catalano V, Turdo A, Di Franco S, Dieli F, Todaro M, Stassi G. Tumor and its microenvironment: A synergistic interplay. Semin Cancer Biol. 2013; 23:522–532. [PubMed: 24012661]

35. Nakao S, Kuwano T, Tsutsumi-Miyahara C, Ueda S, Kimura YN, Hamano S, et al. Infiltration of COX-2-expressing macrophages is a prerequisite for IL-1 beta-induced neovascularization and tumor growth. J Clin Invest. 2005; 115:2979–2991. [PubMed: 16239969]

36. Vasioukhin V, Degenstein L, Wise B, Fuchs E. The magical touch: genome targeting in epidermal stem cells induced by tamoxifen application to mouse skin. Proc Natl Acad Sci U S A. 1999; 96:8551–8556. [PubMed: 10411913]

37. Driessens G, Beck B, Caauwe A, Simons BD, Blanpain C. Defining the mode of tumour growth by clonal analysis. Nature. 2012; 488:527–530. [PubMed: 22854777]

38. Lao HC, Akunda JK, Chun KS, Flake GP, Yuspa SH, Langenbach RJ. Genetic ablation of cyclooxygenase-2 in keratinocytes produces a cell autonomous defect in tumor formation. Carcinogenesis. 2012

39. Brown K, Quintanilla M, Ramsden M, Kerr IB, Young S, Balmain A. v-ras genes from Harvey and BALB murine sarcoma viruses can act as initiators of two-stage mouse skin carcinogenesis. Cell. 1986; 46:447–456. [PubMed: 3015415]

40. Rundhaug JE, Simper MS, Surh I, Fischer SM. The role of the EP receptors for prostaglandin E2 in skin and skin cancer. Cancer Metastasis Rev. 2011; 30:465–480. [PubMed: 22012553]

41. Furstenberger G, Gross M, Marks F. Eicosanoids and multistage carcinogenesis in NMRI mouse skin: role of prostaglandins E and F in conversion (first stage of tumor promotion) and promotion (second stage of tumor promotion). Carcinogenesis. 1989; 10:91–96. [PubMed: 2910536]

Implications

Cox-2 gene deletion demonstrates that intrinsic COX-2 expression in initiated keratinocytes is a principal driver of skin carcinogenesis; lipidomic analysis identifies likely prostanoid effectors.
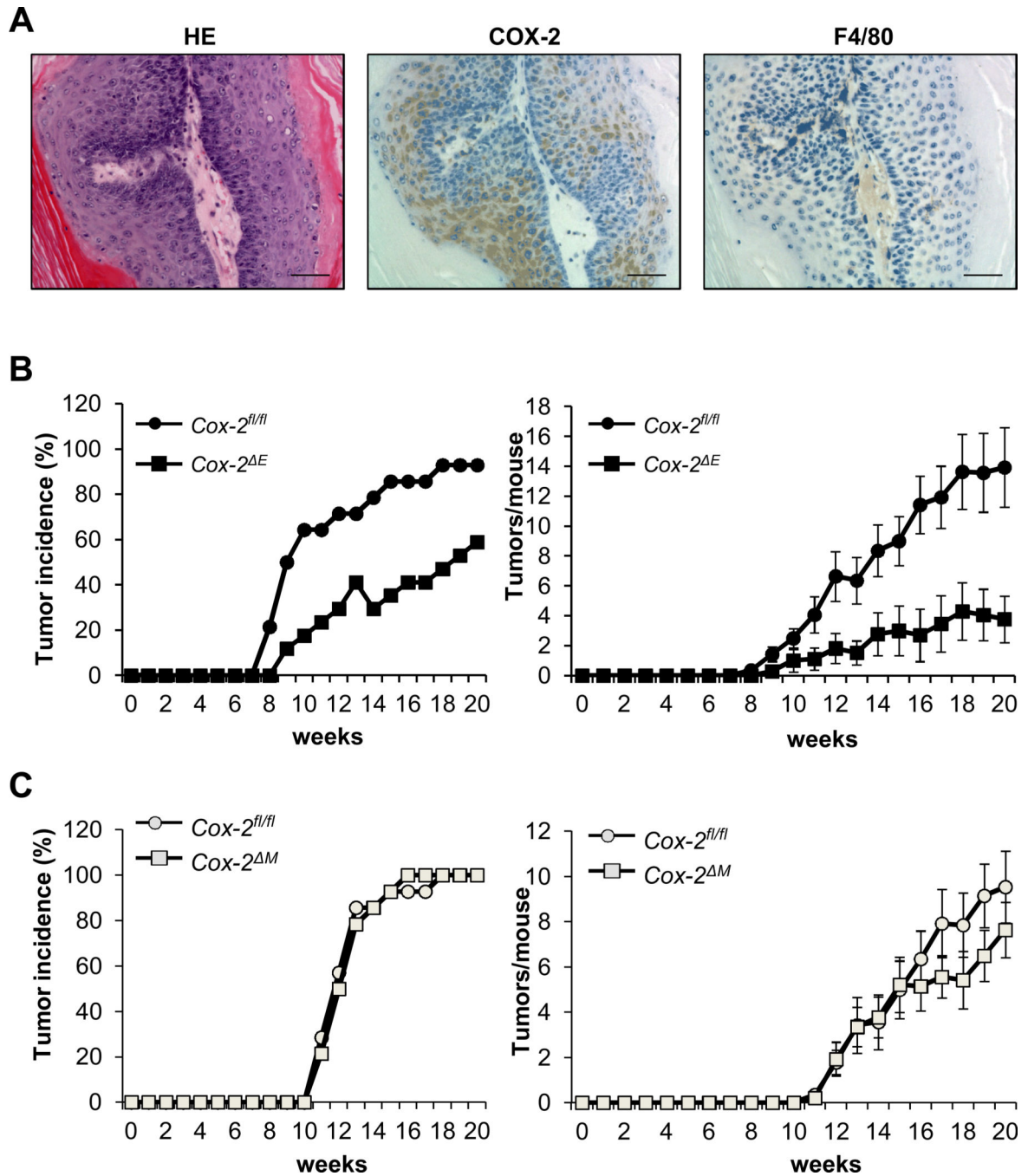
Figure 1. Epidermal keratinocyte-specific *Cox-2* gene deletion reduces DMBA/TPA-induced mouse skin papilloma formation; in contrast myeloid cell-specific *Cox-2* deletion has no effect on DMBA/TPA-induced skin tumor induction

(**A**) DMBA/TPA-induced skin papilloma sections rom a *Cox-2^fl/fl* mouse stained for H&E, COX-2 or F4/80. Scale bars: 50μm. (**B**) *Cox-2* ^E^ mice (n = 20) and *Cox-2^fl/fl* littermates (n = 17) were subjected to DMBA/TPA skin cancer induction. Left panel, the tumor incidence difference between *Cox-2* ^E^ and their *Cox-2^fl/fl* littermate mice was significant by χ^2 test (*p*<0.05). Right panel, tumor multiplicities; error bars, SEM. Significant differences when comparing these groups were determined by Mann-Whitney *U* test (*p* < 0.05–0.001, week

11–20). **(C)** DMBA/TPA tumor induction in *Cox-2*^{M} (n = 15) and *Cox-2*$^{fl/fl}$ littermate mice (n = 15). Error bars, SEM. No significant differences for tumor incidence (χ^2 test) or tumor multiplicities (Mann-Whitney *U* test) were detectable between the groups.
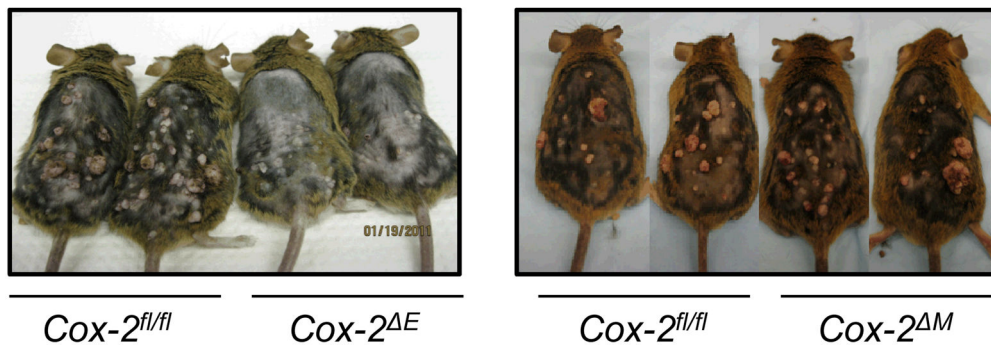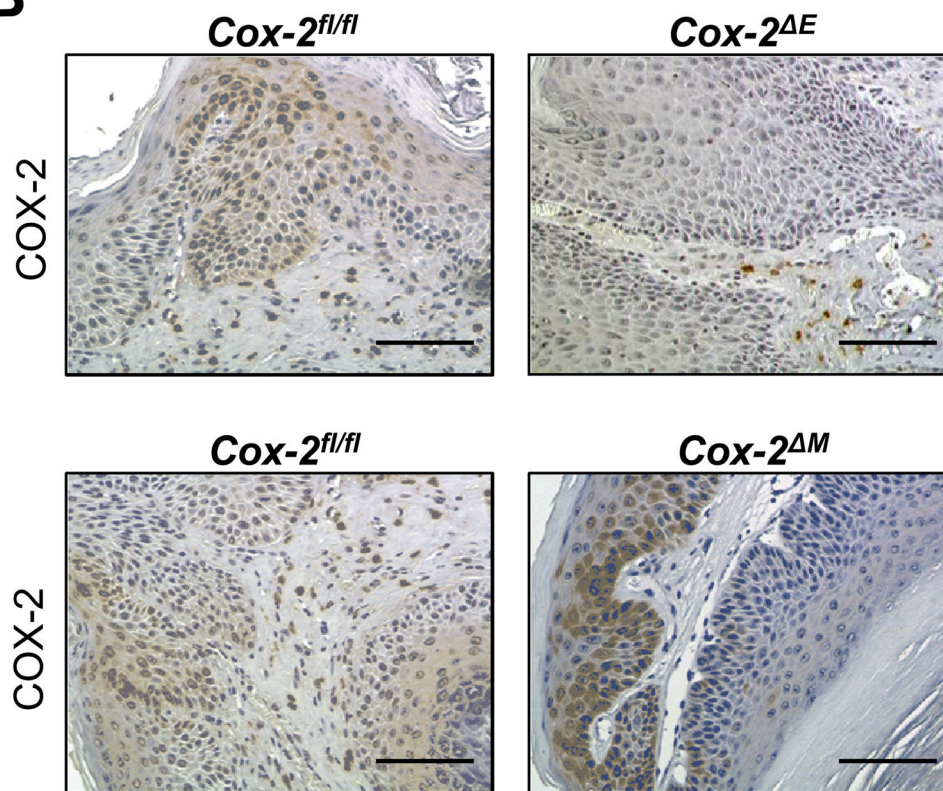
A

$Cox-2^{fl/fl}$ $Cox-2^{\Delta E}$ $Cox-2^{fl/fl}$ $Cox-2^{\Delta M}$

B

Figure 2. DMBA/TPA-induced tumors of $Cox-2^{\Delta E}$ mice are smaller than tumors of $Cox-2^{fl/fl}$ mice, and do not express COX-2 in epithelial tumor cells
(**A**) Left panel; DMBA/TPA-induced tumors on $Cox-2^{\Delta E}$ and littermate $Cox-2^{fl/fl}$ mice (20 weeks of TPA treatment). Right panel; DMBA/TPA-induced tumors on $Cox-2^{\Delta M}$ and littermate $Cox-2^{fl/fl}$ mice (20 weeks of TPA treatment). (**B**) Upper panels; Papillomas from $Cox-2^{\Delta E}$ and littermate $Cox-2^{fl/fl}$ mice were stained for COX-2. Lower panels; Papillomas from $Cox-2^{\Delta M}$ and littermate $Cox-2^{fl/fl}$ mice were stained for COX-2. Scale bars: 100μm.
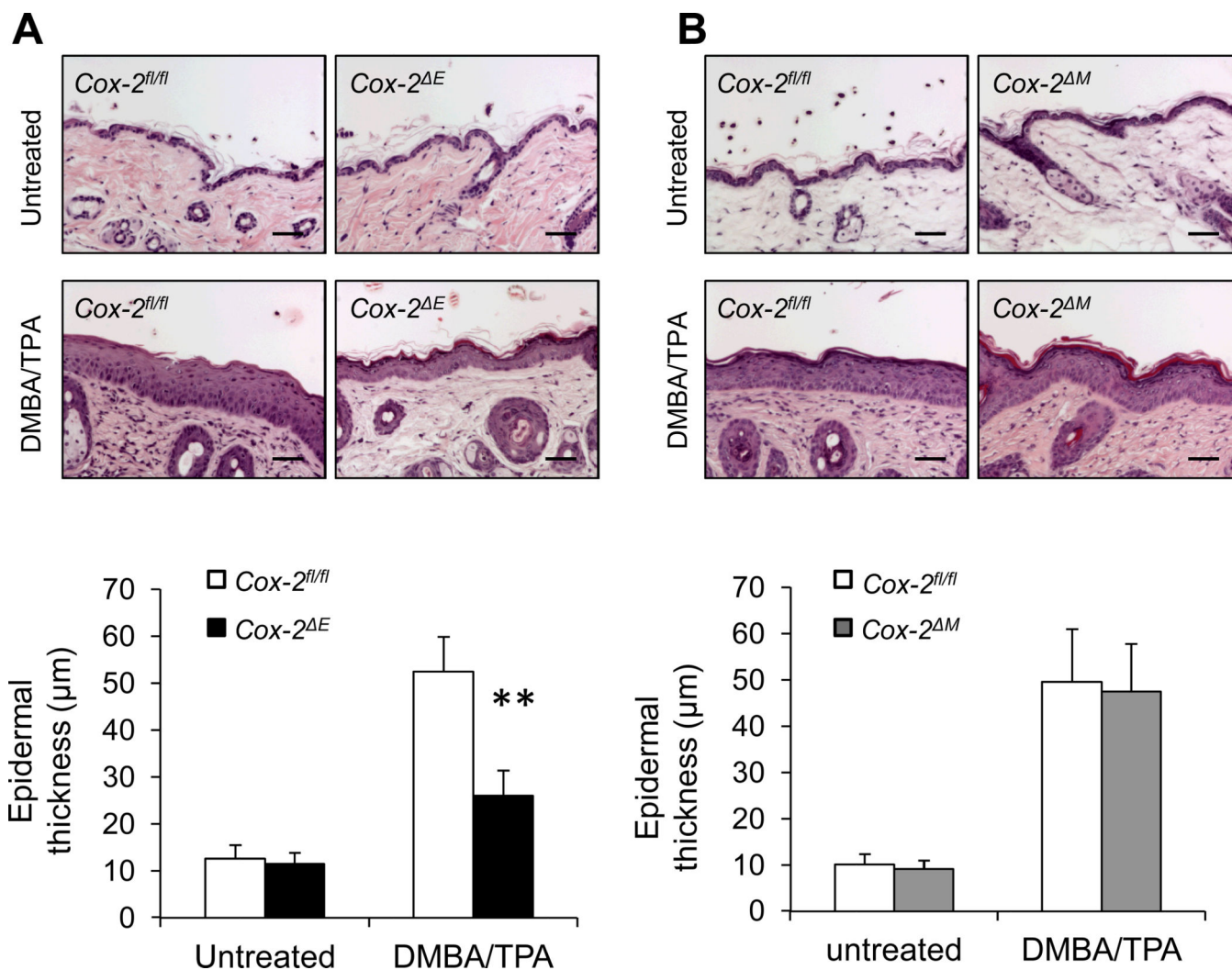
Figure 3. Epidermal hyperplasia is reduced in response to DMBA/TPA treatment in *Cox-2*^{ΔE} mice, but not in *Cox-2*^{ΔM} mice

(**A**) Micrographs (Top): H&E stained skin sections from *Cox-2*^{ΔE} and littermate *Cox-2*$^{fl/fl}$ mice, either untreated or after 20 weeks of DMBA/TPA treatment. Graph (bottom): Epidermal thickness quantification. Error bars, SD. **; $p<0.01$. (**B**) Micrographs (Top): H&E stained skin sections from *Cox-2*^{ΔM} and littermate *Cox-2*$^{fl/fl}$ mice, either untreated or after 20 weeks of DMBA/TPA treatment. Graph (bottom): Epidermal thickness quantification. Twenty fields/mouse, four mice/genotype were counted for all fields. Error bars, SD. n.s., $p>0.05$. Scale bars: 50μm.
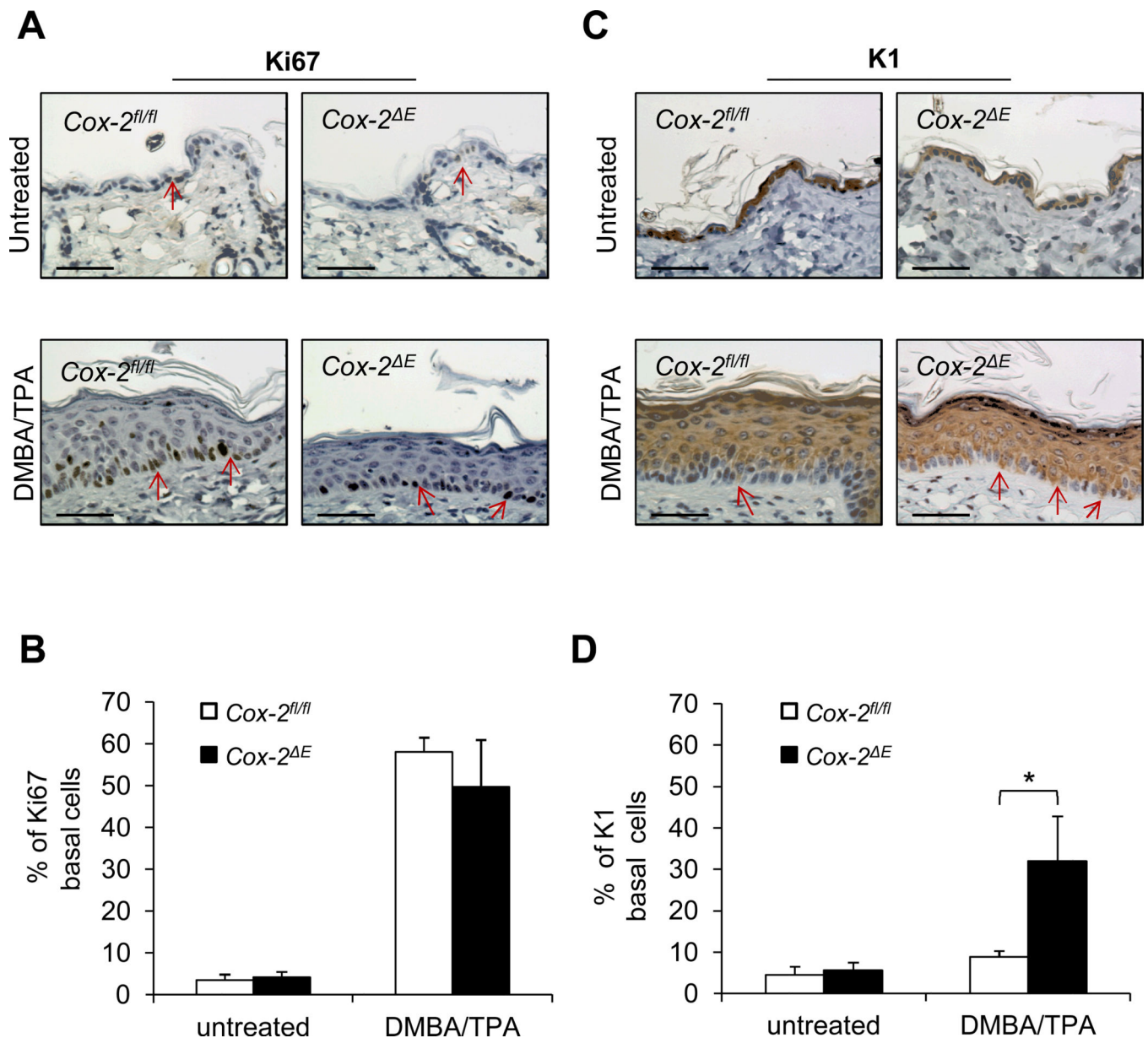
Figure 4. DMBA/TPA-induced skin proliferative responses and epidermal cell differentiation in Cox-2^E mice and Cox-2^{fl/fl} littermate controls

(**A**) Untreated skin samples and skin samples from Cox-2^{fl/fl} and Cox-2^E littermates taken 18 h after the last TPA treatment of the DMBA/TPA-tumor induction protocol, immunostained for Ki67. Arrows indicate Ki67-positive cells. Scale bars: 50μm. (**B**) Percentage of Ki67-positive basal cells in skin samples from untreated mice and DMBA/TPA-treated Cox-2^E and Cox-2^{fl/fl} littermates (**C**) Untreated skin samples and skin samples from Cox-2^{fl/fl} and Cox-2^E littermates taken 18 hours after the last TPA treatment, immunostained for K1. Arrows indicate K1-positive basal cells. Scale bars: 50μm. (**D**) Percentage of K1-positive basal cells in skin samples from untreated mice and DMBA/TPA-treated Cox-2^E and littermate Cox-2^{fl/fl} mice. Ki67-positive and K1-positive basal cells

were determined on at least 4 random areas for each section, 3 sections/mouse and 3 mice/ genotype. Error bars, SD. *, $p<0.05$.
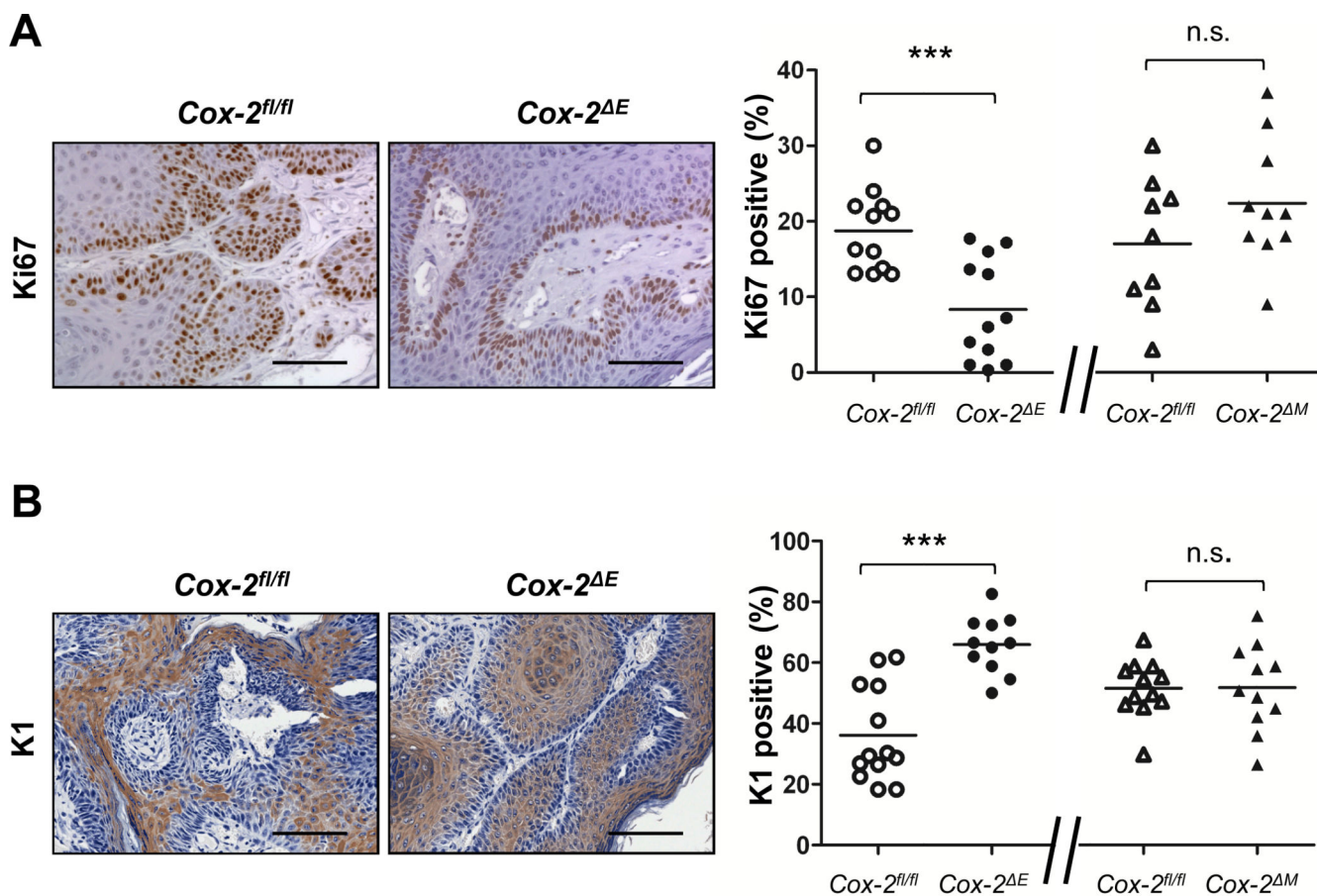
Figure 5. Proliferation and epithelial cell differentiation in DMBA/TPA-induced papillomas from *Cox-2^{ΔE}* mice, *Cox-2^{ΔM}* mice, and their *Cox-2^{fl/fl}* littermates

DMBA/TPA-induced papillomas from at least four mice of each of the four groups were fixed, paraffin embedded, and immunostained for Ki67 and K1. (**A**) Micrographs (Left panels): Ki67-stained papilloma sections from *Cox-2^{ΔE}* and littermate *Cox-2^{fl/fl}* mice. Graphs (right panels): Percentage of Ki67-positive cells in papillomas from *Cox-2^{ΔE}* mice and their *Cox-2^{fl/fl}* littermates, and from *Cox-2^{ΔM}* mice and their *Cox-2^{fl/fl}* littermates. Each data point is the Ki67 value for one papilloma. (B) Micrographs (Left panels): K1-stained papilloma sections from *Cox-2^{ΔE}* and littermate *Cox-2^{fl/fl}* mice. Graphs (right panels): Percentage of K1-positive cells in papillomas from *Cox-2^{ΔE}* mice and their *Cox-2^{fl/fl}* littermates, and from *Cox-2^{ΔM}* mice and their *Cox-2^{fl/fl}* littermates. Each data point is the K1 value for one papilloma, ***, $p < 0.001$. Scale bars: 100μm.
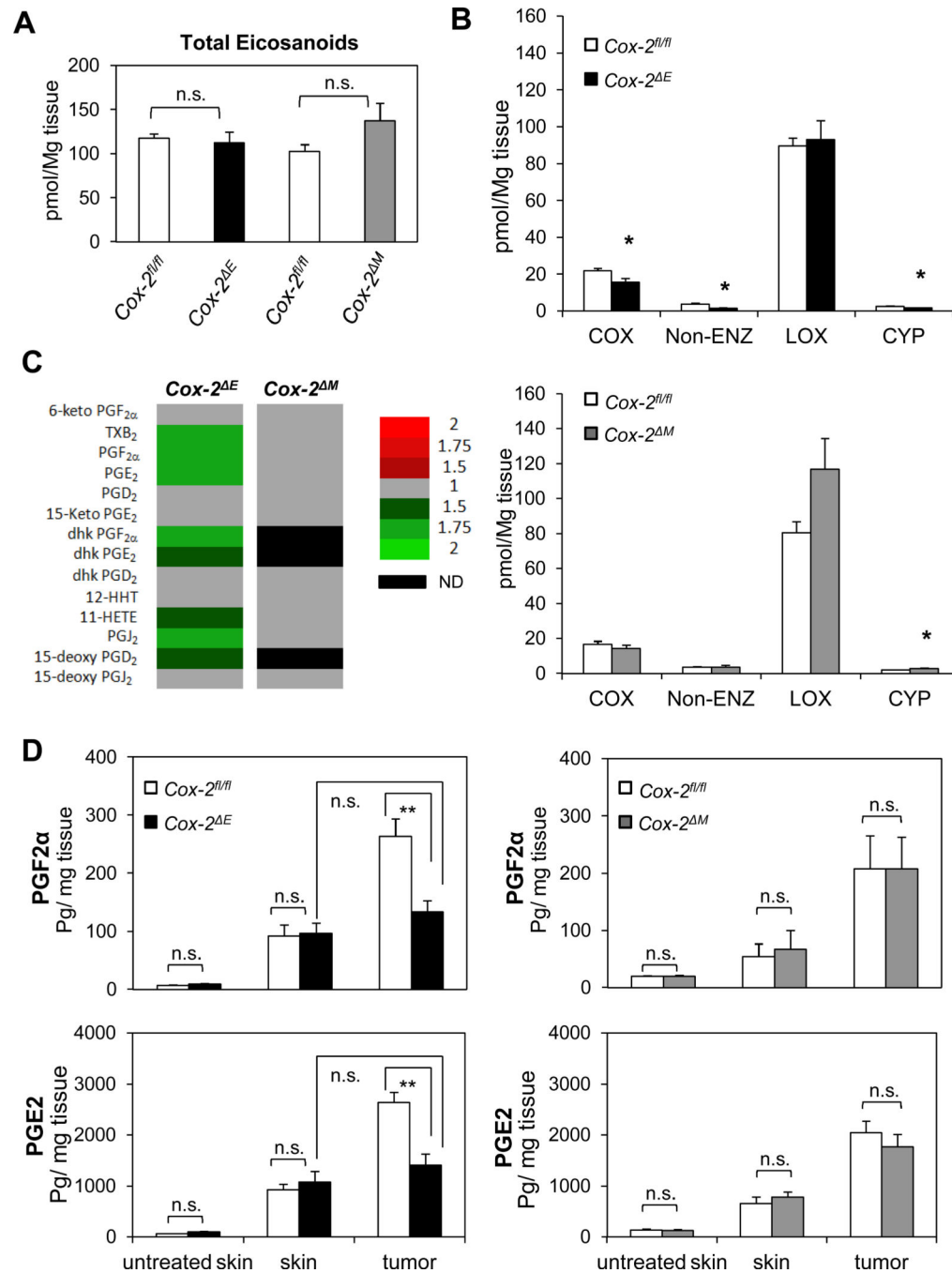
Figure 6. Eicosanoids of skin and tumors from mice with DMBA/TPA-induced skin tumors
(**A**) Total eicosanoids in tumors (n = 12) of DMBA/TPA-treated *Cox-2*[ΔE] mice, their
Cox-2fl/fl littermates (n = 12), *Cox-2*[ΔM] mice (n = 14), and their *Cox-2fl/fl* littermates (n =
13). (**B**) Eicosanoids, separated by pathway of origin (COX-dependent, non-enzymatic,
lipoxygenase-dependent and cytochrome P450 dependent), present in the tumor groups.
Error bars, SD. *, *p*<0.05, determined by a two-tailed student's t-test. (**C**) Heat maps
depicting differences in COX-dependent eicosanoid amounts in *Cox-2*[ΔE] mice, *Cox-2*[ΔM]
mice, and their respective *Cox-2fl/fl* littermates. For each eicosanoid, the amount in tumors

from the *Cox-2* ^{E} or *Cox-2* ^{M} mice was divided by the amount in tumors from their control *Cox-2* $^{fl/fl}$ mice. Green indicates fold-decrease versus *Cox-2* $^{fl/fl}$ control tumors. Red indicates fold increases. Grey, no significant change compared to control *Cox-2* $^{fl/fl}$ tumors. Black (ND), the eicosanoid was either not detected or below the detectable limit. Only eicosanoids significantly different ($p<0.05$) from control littermates are shown. **(D)** $PGF_{2\alpha}$ and PGE_2 amounts detected in untreated skin, in skin from mice treated with DMBA/TPA, and in papillomas from *Cox-2* ^{E} mice, *Cox-2* ^{M} mice, and their cohort littermate *Cox-2* $^{fl/fl}$ control mice (untreated skin from all mice, DMBA/TPA-treated skin of *Cox-2* ^{M} mice and DMBA/TPA-treated skin of control *Cox-2* $^{fl/fl}$ mice, n=6; DMBA/TPA-treated skin of *Cox-2* ^{E} mice, n=8; DMBA/TPA-treated-skin of control *Cox-2* $^{fl/fl}$ mice, n=7). For papillomas, numbers of samples are the same as panels 6A–6C. Error bars, SD. **, $p<0.005$, determined by a two-tailed Student's t-test.
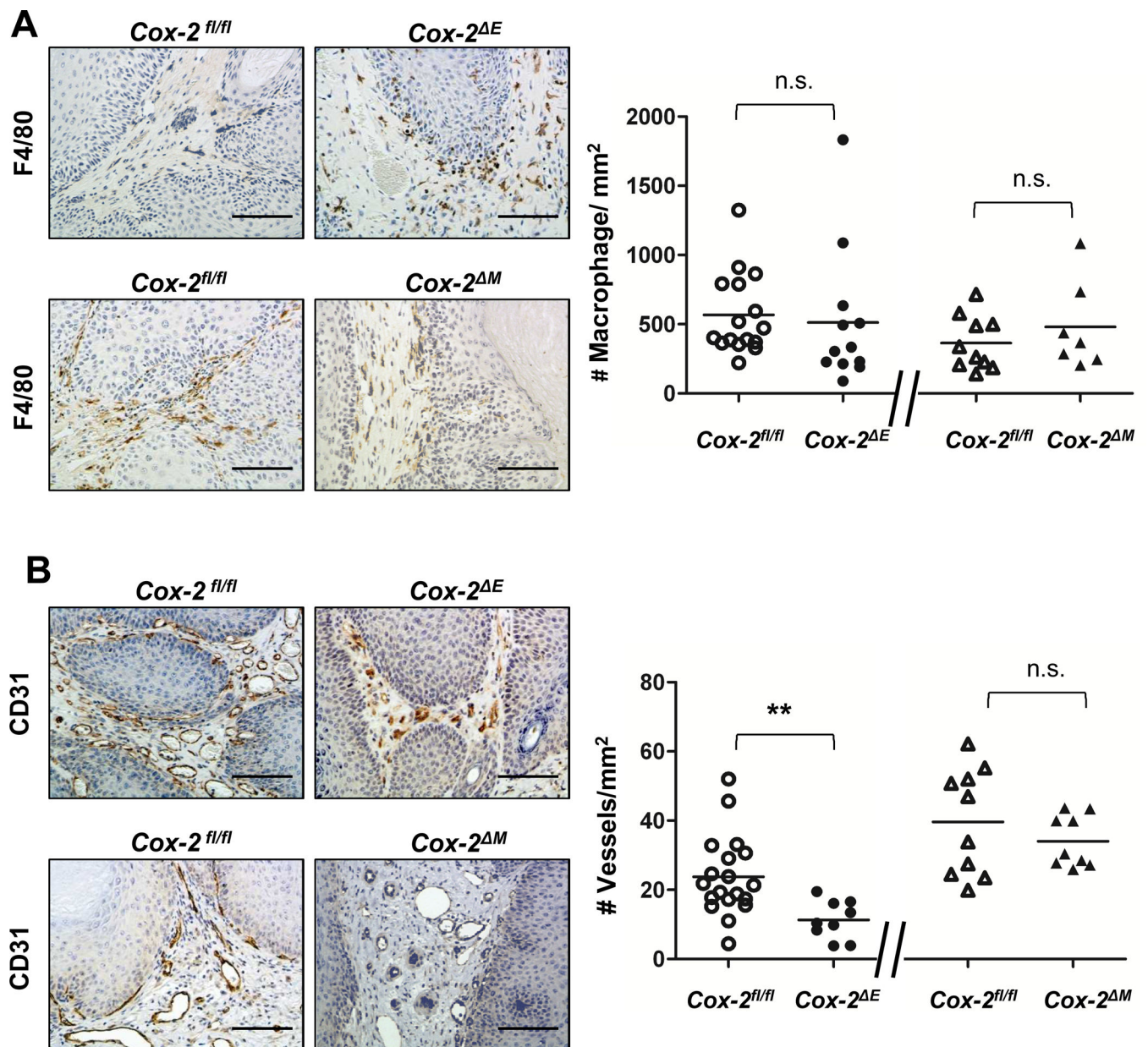
Figure 7. Macrophage infiltration and blood vessel density in DMBA/TPA-induced papillomas from *Cox-2* [E] mice, *Cox-2* [M] mice, and their *Cox-2^{fl/fl}* littermates

DMBA/TPA-induced papillomas from mice of the four groups were fixed, paraffin embedded, and immunostained for F4/80 and for CD31. (**A**) Micrographs (Left panels): F4/80-stained papilloma sections from *Cox-2* [E] mice, *Cox-2* [M] mice, and their respective *Cox-2^{fl/fl}* littermates. Graphs (right panels): Number of F4/80-positive cells/papilloma tumor area for *Cox-2* [E] mice and their *Cox-2^{fl/fl}* littermates, and for *Cox-2* [M] mice and their *Cox-2^{fl/fl}* littermates. Each data point is the F4/80 value for one papilloma. (**B**) Micrographs (Left panels): CD31-stained papilloma sections from *Cox-2* [E] mice, *Cox-2* [M] mice, and their respective *Cox-2^{fl/fl}* littermates. Graphs (right panels): Vessel density in papillomas from *Cox-2* [E] mice and their *Cox-2^{fl/fl}* littermates, and from *Cox-2* [M] mice and their

Cox-2$^{fl/fl}$ littermates. Each data point is the vessel density value for one papilloma. **, *p*<0.01. n.s, *p*>0.05. Scale bars: 100μm.